Journal of Engineering Physics and Thermophysics, Vol. 75, No. 5, 2002

STOCHASTIC-DETERMINISTIC MODELING OF THE DEVELOPMENT OF HYDRODYNAMIC INSTABILITY IN NONISOTHERMAL FILTRATION

M. D. Noskov, A. D. Istomin, and A. G. Kesler

UDC 532.546

Consideration is given to the stochastic-deterministic approach to the modeling of the Saffman–Taylor hydrodynamic instability in nonisothermal filtration of miscible fluids in a porous medium. The numerical model is employed to investigate the dynamics of development of the instability of the case of displacement of a more viscous cold fluid by a less viscous hot fluid in uniformly and nonuniformly permeable media.

Introduction. The Saffman–Taylor hydrodynamic instability develops when a fluid with a lower viscosity displaces a fluid with a higher viscosity from a porous medium or a Hele–Shaw cell [1, 2]. The development of the instability leads to the formation of stochastically bending and branching fingers of the displacing fluid in the region of the displaced fluid. Most investigations, for example [3–8], are devoted to studying the development of the Saffman–Taylor instability when the difference between the displacing and displaced fluids in viscosity is attributed to their properties or to the presence of the substances which are dissolved in them and have an effect on the viscosity. However, the Saffman–Taylor instability can also occur in nonisothermal filtration because of the dependence of the viscosity on the temperature. Study of the hydrodynamic instability in nonisothermal filtration is of both scientific and practical importance, which is related to the prediction of the propagation of contaminants in underground water-bearing horizons, improvement in the efficiency of the extraction of minerals by the method of underground leaching, and solution of a number of chemical-engineering problems.

The present work seeks to study the development of the Saffman–Taylor instability in the case of displacement, from a porous medium, of a cold fluid with a higher viscosity by a hot fluid with a lower viscosity. The development of the instability is governed by the interaction of the temperature and pressure fields. Because of the complexity and nonlinearity of equations which describe nonisothermal filtration, obtaining analytical solutions involves substantial mathematical difficulties. The most efficient method of studying all the stages of development of the instability is numerical modeling. However, deterministic filtration models cannot be employed to describe spontaneous initiation of the instability resulting from the microinhomogeneities of the medium and the fluctuations of fluid motion in the pores. The use of probability methods makes it possible to take into account the stochastic character of development of the instability. To study the growth of the fingers of the displacing fluid one used models employing randomly walking particles [9–11], advance of the displacement front with a probability proportional to the pressure gradient [12–14], and random movement of the lines of equal concentration [15]. However, stochastic models relying on the formal employment of probability regularities make it impossible to investigate the development of hydrodynamic instabilities which are associated with nonequilibrium mass and heat exchange. To model such instabilities we have developed a combined stochastic-deterministic approach which is based on deterministic calculation of mass and heat transfer along stochastically walking streamlines [16–18]. In the present work, it is used to numerically investigate the development of the hydrodynamic instability in nonisothermal filtration.

Formulation of the Problem. Consideration is given to the planned nonisothermal displacement of a cold fluid by a hot fluid from a horizontal heat-insulated bed. The fluid is considered to be incompressible and the porous medium of the bed is considered to be undeformable; the action of gravitational forces is disregarded. The viscosity of the fluid is determined by its temperature. The displacing fluid contains a nonsorbable component which has no effect

Seversk Technological Institute at Tomsk Polytechnic University, Seversk, Russia; email: noskov@hvd.tpu.ru.
Translated from Inzhenerno-Fizicheskii Zhurnal, Vol. 75, No. 5, pp. 108–114, September–October, 2002. Original article submitted December 11, 2001.

1062-0125/02/7505-1139$27.00

on the viscosity. Hydrodispersion is described in the double-porosity approximation [19]. According to this approach, the porous medium is subdivided into flow-through and stagnant pores. In the first case the motion of the fluid is described by Darcy's law [20]. The fluid filling the stagnant pores is not involved in convective motion. The density of the mass flux of the dissolved component between the mobile and immobile parts of the fluid is taken to be in direct proportion to the difference of the corresponding concentrations of the component. The model describes the convective heat transfer and heat conduction in the plane of the bed. Use is made of the approximation of local thermodynamic equilibrium [21], i.e., the temperature of different parts of the fluid and the enclosing rock are equal at each point of the bed.

A system of the equations of single-phase nonisothermal filtration which describes the dynamics of the pressure P, the temperature T, and the concentrations of the dissolved component in the mobile C and immobile C^* parts of the fluid can be written as follows:

$$\operatorname{div} \mathbf{U} = 0 , \tag{1}$$

$$\mathbf{U} = -\frac{k}{\mu (T)} \operatorname{grad} P , \tag{2}$$

$$m_1 \frac{\partial C}{\partial t} = -\operatorname{div} (C\,\mathbf{U}) - \alpha (C - C^*) , \quad m_2 \frac{\partial C^*}{\partial t} = \alpha (C - C^*) , \tag{3}$$

$$\frac{\partial}{\partial t} (cT) = \operatorname{div} (-\mathbf{U}\, c_{\text{liq}} T + \beta \operatorname{grad} T) . \tag{4}$$

The volumetric heat capacity of the medium c is determined by the porosity m and by the heat capacities of the fluid c_{liq} and the enclosing rock c_{s}:

$$c = m c_{\text{liq}} + (1 - m)\, c_{\text{s}} . \tag{5}$$

The thermal conductivity of the medium β depends not only on the thermal conductivities and the volume fractions of the liquid and solid phases but also on the character of their distribution in the pore space. In this work, we employ the Maxwell formula for the thermal conductivity of the porous medium [22]:

$$\beta = \frac{3\beta_{\text{s}} - 2m (\beta_{\text{s}} - \beta_{\text{liq}})}{3 + m (\beta_{\text{s}}/\beta_{\text{liq}} - 1)} . \tag{6}$$

Consideration is given to fluid flow in a rectangular region with dimensions $L_X \times L_Y$ with impermeable boundaries ($\partial P/\partial y = 0$, $y = 0$, L_Y, $0 \le x \le L_X$). On the injection circuit ($x = 0$, $0 \le y \le L_Y$), we prescribe the flow Q of the fluid with temperature T and concentration of the dissolved component C_{in}. On the discharge circuit ($x = L_X$, $0 \le y \le L_Y$), we have free sink ($P = 0$). At the initial instant of time $t = 0$, the temperature in the modeling region is equal to T_0 and the pore space is filled with a fluid containing no dissolved substance ($C_0 = 0$). In calculating the temperature field, we employ the following boundary conditions: the heat flux $c_{\text{liq}} Q T_{\text{in}}$ is prescribed on the injection circuit, the continuous heat flux is set on the discharge circuit, and the side boundaries are heat-insulated ($\partial T/\partial y = 0$).

Formulation of the Numerical Problem. The system of equations (1)–(4) is solved by finite-difference methods. Uniform rectangular spatial and time grids with steps h and τ, respectively, are employed. The values of the grid functions of the pressure $P^n_{i,j}$, the temperature $T^n_{i,j}$, and the concentrations $C^n_{i,j}$ and $(C^*)^n_{i,j}$ on the time layer n at the nodes of the spatial grid (i, j) are found by the method of splitting by physical processes [23]. Computations are carried out in three stages on each time layer. In the first stage, we calculate the distribution of the pressure $P^n_{i,j}$ for constant values of the concentrations and temperature. In the second stage, from the pressure distribution found we calculate the new values of the concentrations of the test component in the flow-through pores $\tilde{C}^n_{i,j}$ and of the tem-

perature $\tilde{T}_{i,j}^n$ which result from the convective mass and heat transfer. In the course of the final stage, we calculate changes in the temperature and the concentration as a result of the conductive heat exchange and mass exchange between the mobile and immobile parts of the liquid phase. As a result of this, we find the values of the temperature $T_{i,j}^n$ and the concentrations $C_{i,j}^n$ and $(C^*)_{i,j}^n$ on the nth time layer.

To calculate the pressure distribution we employ the difference analogs of Eqs. (1) and (2) written in a conservative manner according to the five-point template [24]:

$$\sum_{i',j'} U_{i,j,i',j'}^n = 0 , \tag{7}$$

$$U_{i,j,i',j'}^n = G_{i,j,i',j'}^{n-1} (P_{i,j}^n - P_{i',j'}^n) , \; G_{i,j,i',j'}^n = 2 \left(\frac{\mu (T_{i,j}^n)}{k_{i,j}} + \frac{\mu (T_{i',j'}^n)}{k_{i',j'}} \right)^{-1} , \tag{8}$$

where $U_{i,j,i',j'}^n$ and $G_{i,j,i',j'}^n$ are the fluid flow and the hydraulic conductivity between the nodes (i, j) and (i', j'). Summation in expression (7) is made over all the nodes adjacent to (i, j). Equation (7) is solved for the pressure $P_{i,j}^n$ by the iteration method [23] using the temperature distribution determined on the previous time layer.

The convective mass and heat transfer is calculated based on the method of stochastically walking streamlines [16–18] that begin on the injection circuit and terminate on the discharge circuit. The probability $W_{i,j,i',j'}^n$ of advance of a streamline from the node (i, j) to the adjacent node (i', j') of the calculational grid is taken to be in proportion to the flow $U_{i,j,i',j'}^n$ between the nodes if the fluid flow is directed from the node (i, j) to the node (i', j') and to be equal to zero when the direction of the flow is opposite:

$$W_{i,j,i',j'}^n = (Z_{i,j}^n)^{-1} \, \theta (U_{i,j,i',j'}^n) \, U_{i,j,i',j'}^n , \tag{9}$$

where $Z_{i,j}^n$ is the normalization factor ($Z_{i,j}^n = \sum_{i',j'} \theta(U_{i,j,i',j'}^n) \, U_{i,j,i',j'}^n$; summation is made over all the nodes adjacent to (i, j) and $\theta(x)$ is the step function ($\theta(x) = 1$ for $x > 0$ and $\theta(x) = 0$ for $x \le 0$). The motion of the streamline is initiated at one node of the injection circuit with a probability proportional to the normal component of the filtration rate. At each time step, we construct a single streamline along which the fluid of volume $\Delta V = Q\tau$ is filtered. The size of the time step τ is determined from the condition of equality of ΔV to the volume of the mobile part of the fluid at a single grid node:

$$\tau = m_1 h^2 / Q . \tag{10}$$

For the nodes lying on the streamline the concentration of the component $\tilde{C}_{i,j}^n$ established as a result of convective transfer is taken to be equal to the concentration on the previous time layer $n - 1$ at the node (i', j') which precedes the node (i, j) along the streamline:

$$\tilde{C}_{i,j}^n = C_{i',j'}^{n-1} . \tag{11}$$

The temperature distribution resulting from the convective heat transfer along the streamline is calculated using the difference analog of the law of conservation of energy that is written for the one-dimensional fluid flow in the porous medium in the absence of heat condition:

$$c (\tilde{T}_{i,j}^n - T_{i,j}^{n-1}) = c_{\text{liq}} m_1 (T_{i',j'}^{n-1} - T_{i,j}^{n-1}) , \tag{12}$$

where (i', j') is the node preceding the node (i, j) along the streamline. We take $\tilde{T}_{i,j}^n = T_{i,j}^{n-1}$ and $\tilde{C}_{i,j}^n = C_{i,j}^{n-1}$ for all the nodes beyond the streamline.

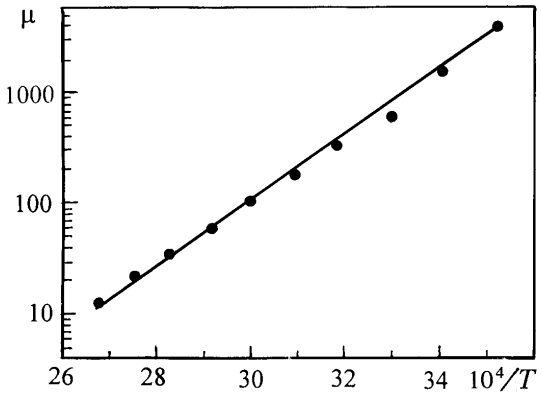

Fig. 1. Viscosity of glycerin μ (mPa·sec) vs. temperature T (K): points, experiment; curve, approximation result.

The values of the concentrations of the dissolved component in the mobile $C^n_{i,j}$ and immobile $(C^*)^n_{i,j}$ parts of the fluid on the time layer n are determined from simultaneous solution of the equations of the kinetics of mass exchange and the mass-balance equation in the system

$$m_1 (C^n_{i,j} - \tilde{C}^n_{i,j}) = \alpha \left((C^*)^n_{i,j} - \tilde{C}^n_{i,j} \right) \tau , \quad m_1 (C^n_{i,j} - \tilde{C}^n_{i,j}) = - m_2 \left((C^*)^n_{i,j} - (C^*)^{n-1}_{i,j} \right). \tag{13}$$

The temperature $T^n_{i,j}$ resulting from conductive heat exchange is calculated based on the difference analog of the heat-conduction equation

$$c (T^n_{i,j} - \tilde{T}^n_{i,j}) = \beta \sum_{i'j'} (\tilde{T}^n_{i',j'} - \tilde{T}^n_{i,j}) \tau h^{-2} , \tag{14}$$

where summation is made over the four nodes adjacent to (i, j). In the case where the time step τ calculated from formula (10) does not satisfy the stability condition [24] of the difference scheme (14) calculation of the pressure field and construction of the streamlines are carried out with a step τ while calculation of the change in the concentration and the temperature on each time layer is carried out N times with a smaller step (equal to τ/N). The value of N is determined from the stability condition.

Thus, in the model proposed to describe convective mass and heat exchange, we employ the stochastic interpretation of Darcy's law. The remaining processes occurring in the system are described based on the corresponding deterministic regularities.

Results and Discussion. The model was employed to study the influence of displacement conditions and of the properties of a porous medium on the development of hydrodynamic instability in displacement of cold glycerin by hot glycerin. The experimental data [25] on the temperature dependence of the glycerin viscosity were approximated by the exponential function $\mu(T) = 1.27 \cdot 10^{-7} \exp (6836/T)$ Pa·sec (the temperature is in K) (Fig. 1). The heat capacity and the thermal conductivity of the glycerin were taken to be $c_{liq} = 2.9 \cdot 10^6$ J/(m^3·K) and $\beta_{liq} = 0.6$ W/(m·K) [26]. The computational experiments were conducted for the following parameters of the bed: $k = 1$ μm^2, $m_1 = 0.27$, $m_2 = 0.11$, $L_X = 40$ m, and $L_Y = 12$ m. The coefficient of mass exchange between the mobile and immobile parts of the fluid corresponded to $\alpha = 0.02$ sec^{-1}. The displacement was modeled for different flow rates Q and temperatures T_{in} of the displacing fluid. The initial temperature of the bed T_0 was equal to 10°C. To study the influence of the heat capacity of the medium on the development of the hydrodynamic instability the computational experiments were conducted for different heat capacities of the enclosing rock. The thermal conductivity of the rock was taken to be $\beta_s = 2$ W/(m·K). The calculations were performed on a 120 × 40-node spatial grid.

A typical result of the modeling of the development of instability is shown in Fig. 2. The pressure redistribution in the medium leads to an accelerated growth of the dominant fingers of the displacing fluid and to the suppression of the growth of the fingers lagging behind. In the process of development, the fingers expand and can split into

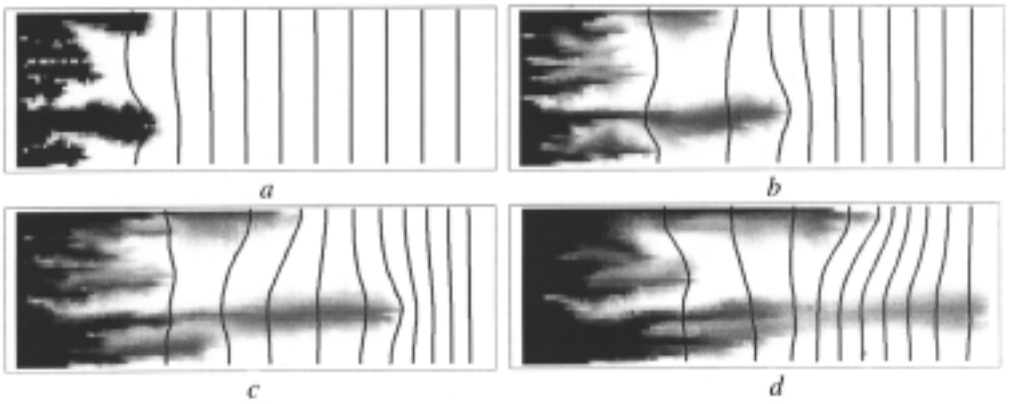

Fig. 2. Results of modeling the development of hydrodynamic instability in displacement of cold glycerin (T_0 = 10°C) by hot glycerin (T_{in} = 60°C) (Q = $4.8\cdot10^{-3}$ m^2/sec, c_s = $1.4\cdot10^5$ J/(m^3·K), Pe = $1.7\cdot10^3$, M = 38, and R = 1.9) for different η: a) 0.1, b) 0.2, c) 0.3, and d) 0.4. The dark color corresponds to the higher temperature; the lines show the isobars.

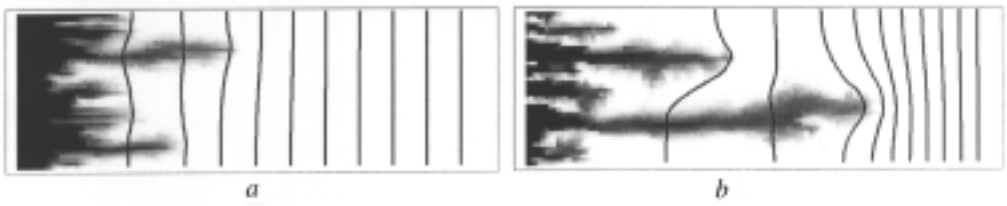

Fig. 3. Results of modeling of displacement for different values of the temperature T_{in} of the injected glycerin [a) 40 (M = 10) and b) 80°C (120)] and the following modeling conditions: Q = $4.8\cdot10^{-3}$ m^2/sec, c_s = $1.4\cdot10^5$ J/(m^3·K), Pe = $1.7\cdot10^3$, R = 1.9, and η = 0.2.

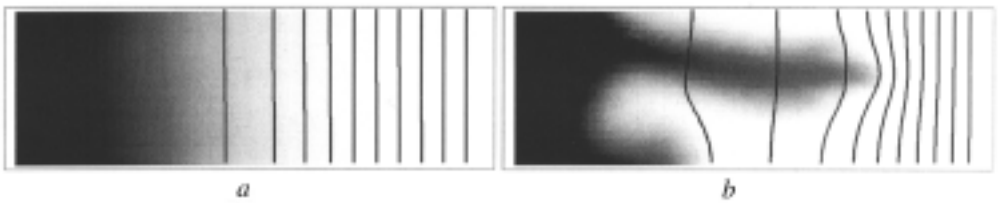

Fig. 4. Results of modeling of displacement for different values of the flow rate [a) Q = $4.8\cdot10^{-6}$ (Pe = 17) and b) $4.8\cdot10^{-5}$ m^2/sec (170)] and the following modeling conditions: T_{in} = 60°C, c_s = $1.4\cdot10^5$ J/(m^3·K), M = 38, R = 1.9, and η = 0.4.

smaller ones. The obtained pattern of growth of the fingers is in qualitative agreement with the results of experimental investigations of the Saffman–Taylor instability [3–6].

The modeling results show that the character of development of the instability is determined by the ratio M of the displaced-fluid viscosity to the displacing-fluid viscosity, the relation between convective heat transfer and heat conduction, and the ratio R between the reduced volumetric heat capacities (heat capacities per unit volume of the medium) of the mobile and immobile parts of the system. The value of the viscosity ratio M depends on the temperatures of the displaced and displacing fluids M = μ(T_0)/μ(T_{in}). The increase in M with increase in the temperature of the injected fluid T_{in} leads to the acceleration of the development of the instability. When the temperatures T_{in} and T_0 are similar the instability does not develop. The displacement patterns obtained for different values of M are shown in Fig. 3.

The relation between convective heat transfer and heat conduction is determined by the Péclet number [27] dependent on the average actual velocity of the fluid flow u = $Q/(L_Y m_1)$, the characteristic dimension of the bed for which one takes its width L_Y, and the thermal diffusivity a = β/c:

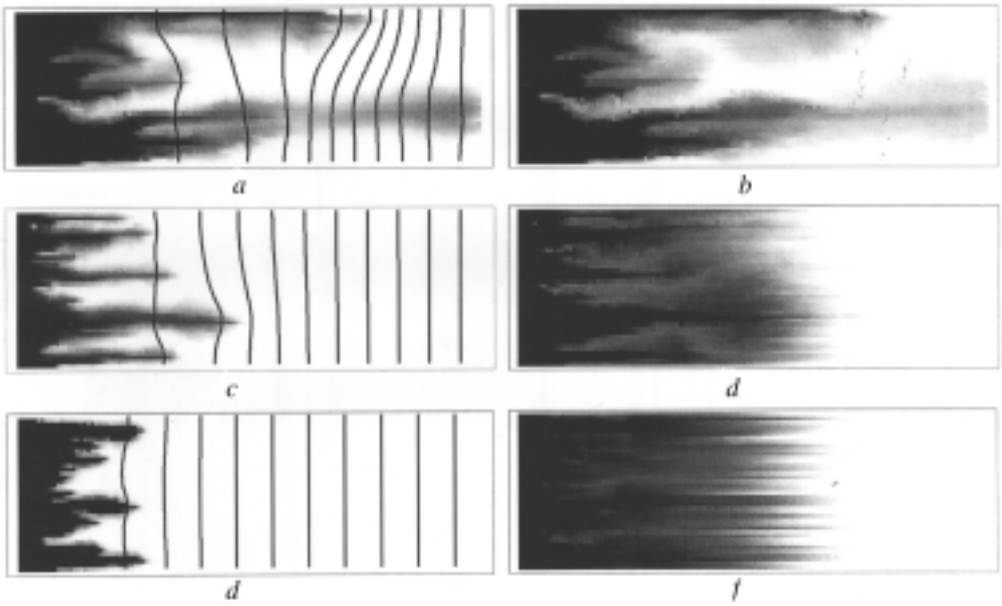

Fig. 5. Results of modeling of displacement for different values of the heat capacity of the rock [a and b) $c_s = 1.4 \cdot 10^5$ (R = 1.9), c and d) $2.8 \cdot 10^6$ (0.4), and e and f) $5.6 \cdot 10^6$ J/(m^3·K) (0.2); a, c, and e) distribution of the temperature and b, d, and f) distribution of the concentration of the test component] and the following modeling conditions: T_{in} = 60°C, $Q = 4.8 \cdot 10^{-3}$ m^2/sec, M = 38, Pe = $1.7 \cdot 10^3$, and η = 0.4.

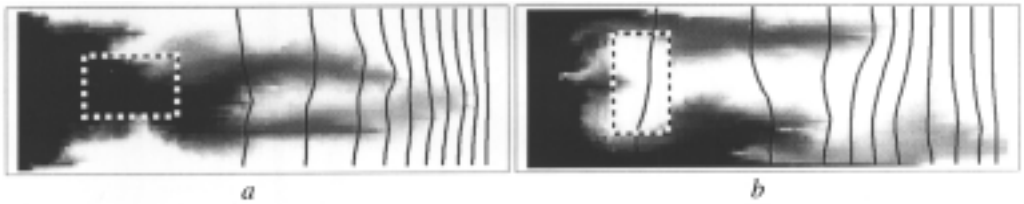

Fig. 6. Results of modeling the development of hydrodynamic instability in a nonuniformly permeable medium [a) high-permeability inclusion, k_{incl}/k = 10; b) low-permeability inclusion; k_{incl}/k = 0.1] with the following modeling conditions: T_{in} = 60°C, $Q = 4.8 \cdot 10^{-3}$ m^2/sec, $c_s = 1.4 \cdot 10^5$ J/(m^3·K), M = 38, Pe = $1.7 \cdot 10^3$, R = 1.9, and η = 0.4. The position of the inclusion is shown as a dashed line.

$$\mathrm{Pe} = uL_Y/a \,. \tag{15}$$

A rapid growth of several fingers of the displacing fluid is observed if the convective heat transfer dominates over the heat exchange (Pe > 100). As the Péclet number decreases because of the heat exchange increasing in importance, the fingers of the displacing fluid expand and their growth is retarded. When the thickness of the fingers becomes comparable to the width of the bed the instability does not develop and we observe a uniform temperate front (Pe < 30). The displacement patterns obtained for different Péclet numbers are shown in Fig. 4.

The value of the ratio R between the heat capacities of the mobile and immobile parts of the system is determined by the heat capacities of the liquid and solid phases and by the porosity of the medium:

$$R = m_1 c_{liq}/(m_2 c_{liq} + (1 - m)\, c_s) \,. \tag{16}$$

When the reduced heat capacity of the mobile fluid is higher than the reduced heat capacity of the immobile part of the system which includes the immobile fluid and the solid phase ($R > 1$), the temperature and concentration distribu-

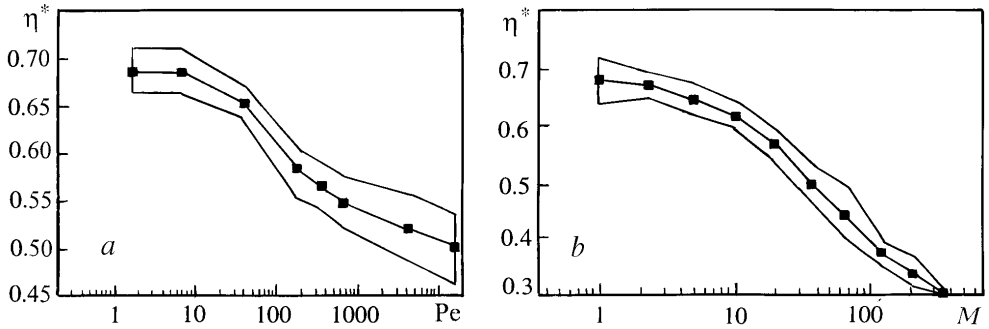

Fig. 7. Ratio η^* of the volume of the displaced fluid to the volume of the flow-through pores at the time of reaching the circuit by the nonsorbable component (result of the averaging over ten numerical experiments) vs. Péclet number Pe (a) and viscosity ratio M of the fluids (b) with the following modeling conditions: $c_s = 1.4 \cdot 10^5$ J/(m^3·K) ($R = 1.9$), $T_{in} = 60^o$C ($M = 38$) (a) and $Q = 4.8 \cdot 10^{-3}$ m^2/sec (Pe = $1.7 \cdot 10^3$) (b). The value of the standard deviation is shown as the frame.

tions of the nonsorbable component are similar (Fig. 5a and b). The increase in the reduced heat capacity of the immobile part of the system leads to the lagging of the temperature fingers behind the concentration fingers and to the expansion of the latter (Fig. 5c and d). When the heat capacity of the mobile fluid becomes much lower than the heat capacity of the immobile part of the system ($R << 1$), the concentration distribution is equalized and the temperature fingers are formed behind the concentration front (Fig. 5e and f).

The presence of the nonuniformity of the permeability of the medium leads to a change in the field of pressure and velocity of the fluid flow. The fingers grow predominantly at sites with the highest velocity of the flow. Figure 6 shows examples of the development of instability when inclusions with a permeability increased or decreased relative to the basic medium are present in the medium. Thus, one can control the development of instability by changing the permeability of the medium. It should be noted that the above effect produced by the nonuniformity of the permeability is also observed in modeling isothermal filtration when the displaced fluid has a high viscosity by virtue of its nature or because of the thickener dissolved in it [14, 18].

An important characteristic of the process of displacement is the ratio η^* of the volume of the displaced fluid to the volume of the flow-through pores at the time of reaching the discharge circuit by the nonsorbable component. In a stable regime of displacement, the quantity η^* is determined by hydraulic dispersion and is close to unity. The development of the instability causes η^* to significantly decrease. Figure 7 shows the quantity η^* as a function of Pe and of the ratio M of the viscosity of the displacing and displaced fluids.

CONCLUSIONS

A stochastic-deterministic model of nonisothermal filtration of miscible fluids has been proposed. The development of hydrodynamic instability in displacement of a cold fluid with a higher viscosity by a hot fluid with a lower viscosity from a porous medium has been investigated numerically. The computational experiments have shown that the rate of development of the instability increases with increase in the ratio M of the displaced-fluid viscosity to the displacing-fluid viscosity and in the Pe number characterizing the relation between convective heat transfer and heat conduction. The character of development of the instability also depends on the ratio R of the reduced heat capacity of the mobile fluid to the reduced heat capacity of the immobile part of the system (the immobile fluid and the solid phase). When the ratio R is more than unity, the fingers of the temperature and concentration of the nonsorbable component dissolved in the displacing fluid are similar. The decrease in the quantity R leads to a decrease in the rate of development of the instability and to the lagging of the temperature fingers behind the concentration fingers and the expansion of the latter. If the quantity R is much less than unity the instability of the temperature front develops against the background of a uniform distribution of the concentration.

This work was carried out with support from the Russian Foundation for Basic Research (grant No. 00-02-16664).

NOTATION

α, coefficient of mass exchange; β, effective thermal conductivity of the medium; β_s, thermal conductivity of the solid phase; β_{liq}, thermal conductivity of the liquid phase; C and C^*, concentrations of the nonsorbable component in the mobile and immobile parts of the fluid; c, effective volumetric heat capacity of the medium; c_{liq}, volumetric heat capacity of the fluid; c_s, volumetric heat capacity of the solid phase; η, ratio of the volume of the displaced fluid to the total volume of the pores; h, period of the spatial grid; k, permeability coefficient of the medium; k_{incl}, permeability coefficient of the inclusion; L_X and L_Y, dimension of the modeling region along the axes of the coordinates X and Y; μ, viscosity; M, ratio of the viscosity of the displaced fluid to the viscosity of the displacing fluid; m, porosity of the medium; m_1 and m_2, flow-through and stagnant porosities of the medium; P, hydrostatic pressure; Pe, Péclet number; R, ratio of the heat capacity of the mobile fluid to the heat capacity of the immobile part of the system; T, temperature; Q, fluid flow through the injection circuit; t, time; τ, period of the time grid; V, volume; $\mathbf{U}$, rate of filtration in the flow-through pores; x, y, Cartesian coordinates. Subscripts: liq, liquid; s, solid; in, inlet; incl, inclusion; 0, initial value.

REFERENCES

1. S. Hill, *Chem. Eng. Sci.*, **1**, 247–253 (1952).
2. P. G. Saffman and G. Y. Taylor, *Proc. Roy. Soc. London, Ser. A*, **245**, 312–329 (1958).
3. R. L. Slobod and R. A. Thomas, *Soc. Petrol. Eng. J.*, **3**, 9–13 (1963).
4. B. Habermann, *Trans. AIME*, **219**, 264–272 (1960).
5. K. S. Sorbie, H. R. Zhang, and N. B. Tsibuklis, *Chem. Eng. Sci.*, **50**, No. 4, 601–616 (1995).
6. H. R. Zhang, K. S. Sorbie, and N. B. Tsibuklis, *Chem. Eng. Sci.*, **52**, No. 1, 37–54 (1997).
7. C. T. Tan and G. M. Homsy, *Phys. Fluids*, **29**, No. 11, 3549–3556 (1986).
8. Y. C. Yortsos and M. Zeybek, *Phys. Fluids*, **31**, No. 12, 3511–3518 (1988).
9. L. Paterson, *Phys. Rev. Lett.*, **52**, No. 18, 1621–1624 (1984).
10. R. B. Selinger, J. Nittmann, and H. E. Stanley, *Phys. Rev. A*, **40**, No. 5, 2590–2601 (1989).
11. H. Siddiqui and M. Sahimi, *Chem. Eng. Sci.*, **45**, No. 1, 163–182 (1990).
12. A. J. DeGregoria, *Phys. Fluids*, **28**, No. 10, 2933–2935 (1985).
13. J. D. Sherwood and J. Nittmann, *J. Physique*, **47**, 15–22 (1986).
14. M. D. Noskov and A. B. Rylin, *Inzh.-Fiz. Zh.*, **73**, No. 2, 267–273 (2000).
15. M. J. King and H. Scher, *Phys. Rev. A*, **41**, No. 2, 874–883 (1990).
16. M. D. Noskov and A. D. Istomin, *Mat. Model.*, **11**, No. 10, 77–85 (1999).
17. M. D. Noskov and A. D. Istomin, *Mat. Model.*, **12**, No. 10, 19–30 (2000).
18. M. D. Noskov, A. D. Istomin, and A. G. Kesler, *Inzh.-Fiz. Zh.*, **75**, No. 2, 69–74 (2002).
19. G. I. Barenblatt and Yu. P. Zheltov, *Dokl. Akad. Nauk SSSR*, **132**, No. 3, 545–548 (1960).
20. L. Lukner and V. M. Shestakov, *Modeling of Migration of Underground Water* [in Russian], Moscow (1986).
21. M. G. Alishaev, M. D. Rozenberg, and E. V. Teslyuk, *Nonisothermal Filtration in Oil-Field Development* [in Russian], Moscow (1985).
22. V. N. Kobranova, *Petroleum Physics* [in Russian], Moscow (1986).
23. S. K. Godunov and V. S. Ryaben'kii, *Difference Schemes* [in Russian], Moscow (1977).
24. A. A. Samarskii, *Introduction to the Theory of Difference Schemes* [in Russian], Moscow (1971).
25. N. B. Vargaftik, *Handbook of the Thermophysical Properties of Gases and Liquids* [in Russian], Moscow (1963).
26. N. B. Vargaftik, L. P. Filippov, A. A. Tarzimanov, and E. E. Totskii, *Handbook of the Thermal Conductivity of Liquids and Gases* [in Russian], Moscow (1990).
27. L. G. Loitsyanskii, *Mechanics of Liquids and Gases* [in Russian], Moscow (1970).